

Three-dimensional Electro-Fenton Oxidation of Landfill Leachate Concentrates Using MnO₂-doped TiO₂-coated Granular Activated Carbon as Catalytic Particle Electrodes

Jinxiang Fu¹, Xiang He^{1,*}, Jinghai Zhu², Wenyi Gu¹, Xiaoxi Li¹

¹ School of Municipal and Environmental Engineering, Shenyang Jianzhu University, Shenyang 110168, China

² School of Public Health, China Medical University, Shenyang 110000, China

*E-mail: syzhexiang@163.com

Received: 27 January 2018 / Accepted: 29 March 2018 / Published: 10 May 2018

A composite catalytic particle electrode (CPE) consisting of granular activated carbon (GAC)-coated MnO₂-doped TiO₂ (Mn-Ti-GAC) was prepared and applied in a three-dimensional electro-Fenton (3DEF) system to treat nanofiltration concentrates (NFC) from a municipal landfill in northeast China. The CPE samples were characterized by XRD, SEM-EDS, BET, and XPS analyses. The stability, reusability, and generation of hydroxyl radicals ($\cdot\text{OH}$) on the Mn-Ti-GAC particles in the 3DEF system were compared with other reported CPEs. Following optimization of the reaction conditions, including a current density of 15 mA/cm², Fe²⁺ concentration of 1 mmol/L, CPE concentration of 200 g/L, and an initial pH of 3, the removal efficiencies of the chemical oxygen demand and ammonia nitrogen were 84.68 % and 81.3 %, respectively. The refractory organic (i.e., humic acid and fulvic acid) removal efficiency was higher than that of the hydrophilic fraction due to the type of pore distribution in the Mn-Ti-GAC particles. The 24h-LC₅₀ biotoxicity of the NFC to *Artemia salina* decreased rapidly following treatment, and the five-day biological oxygen demand (BOD₅)/COD increased from 0.002 to 0.296 at the end of the reaction.

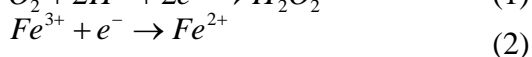
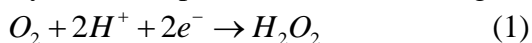
Keywords: Landfill leachate concentrates; Three-dimensional electro-Fenton; Mn-doped TiO₂; Dissolved organic matter; Biotoxicity

1. INTRODUCTION

Although the 3Rs (reduce, reuse, recycle) have become increasingly popular in China to address the issue of solid waste generation, landfills are still the principal method for municipal solid waste disposal because of its economy. Landfill leachate is an extremely complex type of wastewater generated during the biochemical transformation of waste [1,2,3]. Membrane separation techniques

like membrane bio-reactors (MBR) [4], nanofiltration (NF) [5], and reverse osmosis (RO) [6] have been widely used in the treatment of landfill leachate in order to meet China's national discharge standard (GB16889-2008). Landfill leachate concentrates have been produced by membrane interception, and these concentrates usually have low five-day biological oxygen demand (BOD₅)-to-chemical oxygen demand (COD) ratios and high refractory organic contents including humic acid (HA) and fulvic acid (FA) [7,8]. Although recirculating these concentrates into landfills was considered to be economical, such an approach may lead to the accumulation of ammonia nitrogen (NH₃-N) and metal ions, which increase the biological processing load and decrease the efficiency of the membrane processes. For these reasons, it is thus necessary to develop alternative methods to manage landfill concentrates.

Advanced oxidation processes (AOPs) have recently been reported for the treatment of highly concentrated organic wastewater-like concentrates [3,9,10,11]. One of such AOPs is three-dimensional electro-Fenton (3DEF), which has received considerable attention because of its high efficiency and low operating costs. In 3DEF systems, H₂O₂ is generated at carbonaceous cathodes via Reaction (1) when O₂ or air is fed into the reactor, which avoids the potential risks from the transport, storage, and handling of H₂O₂ directly [12]. Moreover, Fe²⁺ is continuously regenerated via Reaction (2) which effectively avoid the production of iron sludge [13].



Particle-type electrodes using 3DEF systems have progressed significantly since their first proposal. GAC is a particle electrode with a high adsorption capacity, very high BET surface area, and macro-size pore distribution; it is also relatively inexpensive [14]. In addition, the pore volume reduction of GAC is proportional to the amount of GAC in the catalyst, which means that the pores are not blocked by the agglomeration of TiO₂ particles [11]. However, pure GAC has been shown to have a weak electrochemical oxidation capacity and is inefficient at producing hydroxyl radicals, ·OH [15]. In order to overcome these shortcomings, catalyst-coated GACs with strong ·OH production capacities have received attention. Recently, TiO₂ was demonstrated to contribute to the oxidation reaction in an electrocatalytic oxidation system [16]. Additionally, Li [15] found that transition metal oxide-doped TiO₂ in an electrochemical system could significantly improve the electro-generation of ·OH and thereby enhance the oxidation of pollutants relative to pure TiO₂ catalysts. In 3DEF technology, however, much less attention has been given to Mn-doped TiO₂ as a catalyst on GAC and the oxidation of pollutants in highly concentrated organic wastewater.

In this study, we developed a composite CPE in which MnO₂-doped TiO₂ was impregnated into a GAC carrier by a one-step sol-gel method. The resultant product was then used in a 3DEF system to treat NFC. The physical properties, catalytic ability, and service life of the CPE were investigated and characterized. Additionally, the effects of current density, initial pH, CPE concentration, and the concentration of ferrous ions on the 3DEF performance were evaluated to determine the optimal reaction conditions. The effect of the 3DEF process on COD; nitrogen; dissolved organic matter (DOM), including HA, FA, and hydrophilic fraction (HyI); metals (Cr, As, Hg, Cd, Se); and biotoxicity were also investigated. Finally, the degradation mechanism of organic matter in the 3DEF system was discussed.

2. EXPERIMENTAL

2.1 Materials

The NFC samples were collected from a municipal landfill plant (Shenyang China) that has been in operation for thirteen years. The landfill leachate had been treated via a submerged membrane bioreactor-NF-RO process. The concentrates were collected and stored in a refrigerator at 4 °C before use in the 3DEF treatment tests. The NFC characteristics include: COD, 6815.42±32.5 mg/L; BOD₅, 12.53±1.05 mg/L; NH₃-N, 65.8±4.72 mg/L; total ammonia (TN), 1446.21±7.29 mg/L; pH 6.2–7.3; Fe³⁺, 5.62±0.7 mg/L.

Ethanol, acetic acid (36–38 wt.%), nitric acid, tetrabutyl orthotitanate (TBOT, C₁₆H₃₆O₄Ti), manganese (II) nitrate (50 % solution), NaOH and FeSO₄ were obtained from Sinopharm Chemical Reagent Co. Ltd., China. All chemicals were of analytical grade and used as received without further purification. GAC (average size: ~4–6 mm; specific surface area: ~600 m²/g) was purchased from Henan Lvyuan Water Treatment Technology Co. Ltd., China.

2.2 Preparation of CPEs

GAC was initially washed with distilled water and then washed again several times during ultrasonication for 30 min before use. The GAC was then dried at 105 °C for 24 h.

Mn-Ti-GAC was prepared using a one-step sol-gel method, for which the optimal conditions were determined through orthogonal experiments. TBOT (20 mL) was added to absolute ethanol (40 mL) (Solution A). Acetic acid (5 mL), Mn(NO₃)₂ (0.7 mL), HNO₃ (5.3 mL), and deionized water (5 mL) were dissolved in absolute ethanol (20 mL) (Solution B). Solution B was then added dropwise into Solution A, followed by the addition of GAC (55 g) over a period of 3 h at 25 °C. The mixture was then dried at 105 °C for 12 h. The as-prepared Mn-Ti-GAC particles were annealed at 500 °C for 2 h.

The preparation of Ti-GAC was similar to that of Mn-Ti-GAC except that the added Mn(NO₃)₂ concentration was replaced with distilled water. GAC (55 g) was then added to the mixed solutions, dried at 105 °C for 12 h, and annealed at 500 °C for 2 h. Mn-GAC was prepared by an impregnation method. Specifically, GAC (55 g) was added to a Mn(NO₃)₂ solution (100 mL, 0.1 mol/L), which was then dried at 105 °C for 12 h followed by annealing at 500 °C for 2 h.

2.3 Toxicity testing

Artemia salina (brine shrimp) has gained popularity as a test organism because of its ease of culture, short generation time, diverse distribution, and the commercial availability of its dormant eggs (cysts). Acute toxicity of the NFC following treatment was tested using *Artemia salina* according to Aline [17] with some modifications. A solution of standard artificial seawater of 35±1‰ was used as the incubation medium for the *Artemia salina* cysts. Instar II–III larvae of *Artemia salina* (n = 10) were placed into 50 mL beakers, which were then filled with 10 mL of each concentration (~5–100 %) or

the control medium. The beaker was then illuminated with a 20 W fluorescent lamp. Each experiment was replicated five times. The salinity of all the dilutions was corrected to be identical to that of the incubation medium with the direct addition of synthetic sea salt. After 24 h of exposure, the number of dead organisms was observed and noted, and the mean lethal concentration (LC_{50}) was calculated by the probability unit method.

2.4 Reaction quenching study

In order to identify the impact of CEPs packed in the 3DEF system, quenching tests were performed to measure the generation of $\cdot OH$ present in the reaction system. Tertiary butanol was used as quenching reagent for $\cdot OH$ via a dehydrogenation reaction [18]. Different mass concentrations (0, 3, 5, 10, 15, and 30 mg/L) of tertiary butanol were added to various 3DEF systems filled with different CEPs (named 3DEF-GAC, 3DEF-Mn-GAC, 3DEF-Ti-GAC, 3DEF-Mn-Ti-GAC, adding Fe^{2+} , voltage application, and aerating), a traditional anodize system (2D) (without adding CEPs, Fe^{2+} , aerating, only voltage application), a three-dimensional electrochemical system (3D-Mn-Ti-GAC) (adding Mn-Ti-GAC particles named 3D-Mn-Ti-GAC, voltage application, and aerating without adding Fe^{2+}), and an electro-Fenton system (2D/F) (without CEPs, adding Fe^{2+} , aerating, and voltage application). The COD removal efficiency was measured to characterize the degradation contribution of $\cdot OH$ and the CEP reaction mechanism.

2.5 Analytical methods

The CPE morphologies were observed by a scanning electron microscopy-energy dispersive X-ray (SEM-EDS) apparatus (JEOL JSM-7500F, Japan), an X-ray diffractometer (XRD, Shimadzu S-7000, Japan), a BET surface area analyzer (Quadrasorb SI/AUtosorb-IQ-MP-2046, UAS), and an X-ray photoelectron spectroscopy (XPS) spectrometer (Thermo Xi-250, UAS). The COD, BOD_5 , NH_3-N , TN, nitrite nitrogen (NO_2-N), and nitrate nitrogen (NO_3-N) were determined according to standard methods [19]. The DOM in the NFC before and after 3DEF treatment was fractionated into HA, FA, and HyI using the method described by Zhang [8]. The total organic carbon (TOC) was measured using a Shimadzu TOC-VCPH analyzer. The influent and effluent samples were digested with nitric-perchloric acid, and the change in the metal concentration (Cr, Cd, Pb, Hg, and As) was measured using inductively coupled plasma mass spectrometry (ICP-MS) (Agilent 7500cx, USA).

2.6 Experimental procedures

The 3DEF reaction was conducted in a cylindrical electrochemical cell ($15 \times 11 \times 11$ cm). Experiments were conducted in batch mode with aeration using 1.5 L of the NF leachate concentrate. The anode and cathode were Ti-Ru-Ir and stainless steel, respectively. Both electrodes were used with an immersed area of 55 cm^2 . To ensure adsorption equilibrium, the CPEs were added into a solution of NFCs prior to the electrochemical oxidation treatment and the vessel was shaken for 48 h until the

COD value remained unchanged. The adsorption-saturated CPEs were then transferred for electrolysis. A direct current electric source (Yaguang HY1711-3S, China) was connected between the plates, and air was bubbled from the bottom of the apparatus (4.5 L/min) to provide oxygen and stir the liquor. Samples were collected at fixed time intervals before adjusting the pH to 10 and filtering with 0.45 μm filter paper. The samples were stored at 4 $^{\circ}\text{C}$ for further analysis.

3. RESULTS AND DISCUSSION

3.1 CPE physical characterization

The surface morphology of the CPEs was observed with SEM. As seen in Fig. 1(a), the GAC surface possessed significant cracks and a macroporous structure. The CPE surface became smooth when coated with the catalytic particles and the irregular pores disappeared. The GAC surface differed in form and coverage with different metal oxides. For instance, manganese oxide showed aggregation on the edge of the GAC pores (Fig. 1(b)). This coating lacked active sites and was easily removed, which further reduced active site formation. By comparison, the titanium oxide catalyst layer (Fig. 1(c) and (d)) formed a flake-like structure and was covered with many pores, demonstrating an obvious metallic crystal layer. The structure of the Mn-Ti-GAC particles was similar to that of Ti-GAC in that the presence of metallic crystal layers was obvious. The surface and pores of the Mn-Ti-GAC particles were covered with nanoparticles, and the agglomerated structure of Mn-Ti-GAC was more distinct than that of Ti-GAC. EDS was used to characterize the elemental composition of the CEPs (Table 1). In all CEPs, C and O were the dominant elements. Additionally, elemental Mn and Ti were detected in Mn-Ti-GAC, indicating that these two metals were successfully coated onto the GAC substrate. It is noteworthy that the Ti-to-Mn mass ratio of Mn-Ti-GAC was 10.93; the relatively low proportion of Mn may result from Mn entering the TiO_2 crystal and forming a solid solution.

As shown in Table 1, the specific surface area and pore volume of GAC were higher than those of the GAC-coated electrodes. Catalytic particles covered some of the external and internal pores of GAC, thereby reducing its surface area. Meanwhile, $V_{\text{mic}}/V_{\text{tot}}$ decreased due to blockage of the micropores by metallic oxides, which increased the size and number of mesopores on the GAC surface. Furthermore, on account of the similar ionic radius between Ti^{4+} (0.53) and Mn^{4+} (0.54), Mn^{4+} was able to replace Ti^{4+} and form a $\text{MnO}_2\text{-TiO}_2$ solid solution, which inhibited nano- TiO_2 crystal grain formation and growth. Hence, the crystal grain size decreased and the specific area of Mn-Ti-GAC increased, which is why this material possessed a larger specific surface area than Ti-GAC.

The XRD analysis in Fig. 2 indicates the differences in the diffractograms of the three types of particles. The catalyst in the Mn-GAC and Ti-GAC CPEs was primarily composed of MnO_2 (JCPDS Card No. 43-1455) and rutile TiO_2 (JCPDS Card No.88-1173), respectively. However, the catalyst in Mn-Ti-GAC is primarily composed of anatase TiO_2 (JCPDS Card No. 21-1272), and no Mn oxides were evident in its XRD pattern, which contrasts the results of EDS (Table 1). To rationalize this observation, we presume that doping elemental Mn forms an amorphous compound or enters the TiO_2 lattice during the sol-gel casting method and tightly associates with anatase TiO_2 .

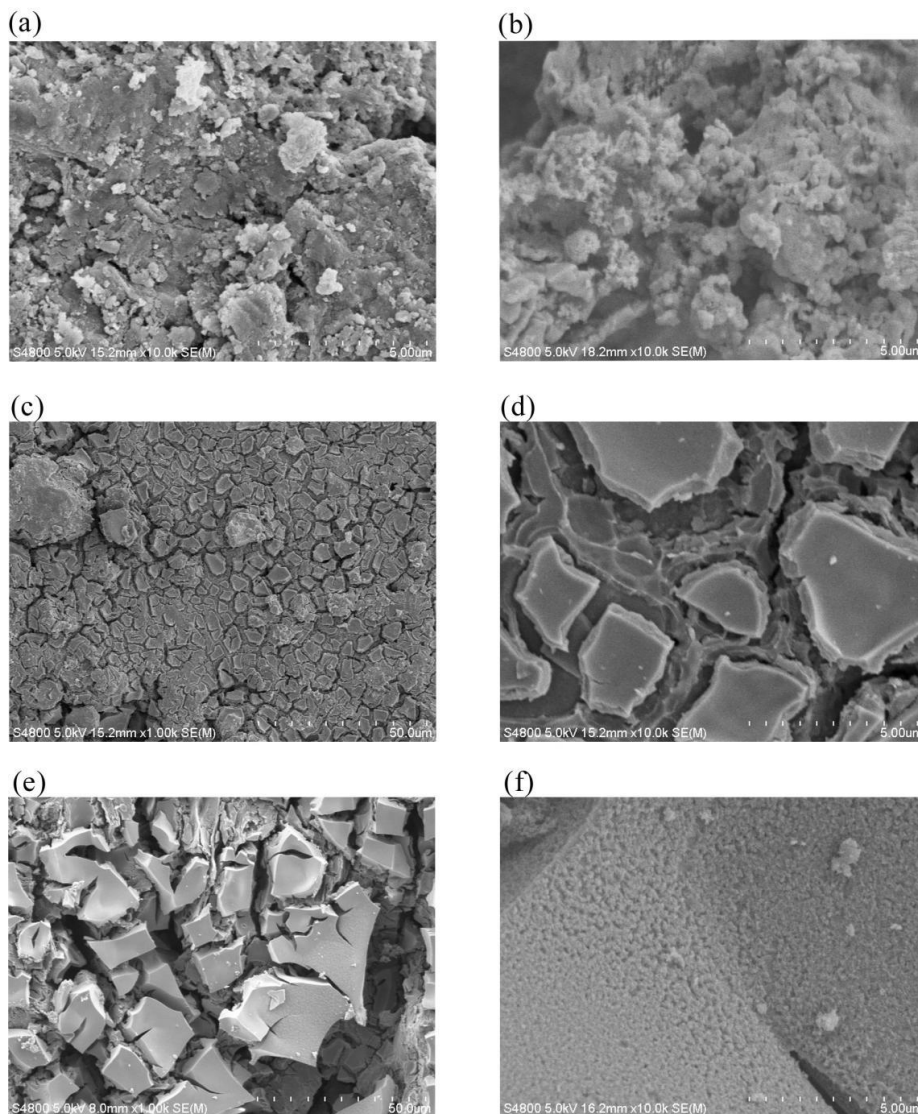


Figure 1. SEM images of CPEs: (a) GAC; (b) Mn-GAC; (c, d) Ti-GAC; and (e, f) Mn-Ti-GAC.

Table 1. Properties of the as-synthesized CPEs

Parameters	GAC	Mn-GAC	Ti-GAC	Mn-Ti-GAC
Specific surface area(m ² /g)	705.46	600.82	563.91	581.37
Average pore size(nm)	2.07	1.96	1.86	1.89
Total pore volume(V _{tot})(cm ³ /g)	0.432	0.408	0.376	0.383
V _{micro} (V _{mic})(cm ³ /g)	0.414	0.381	0.328	0.331
V _{mic} /V _{tot} (%)	95.83	93.38	87.23	86.42
C(mass ratio %)		56.31	53.48	55.61
O(mass ratio %)		19.78	21.61	23.08
Mn(mass ratio %)		16.79		4.7
Ti(mass ratio %)			12.95	0.43

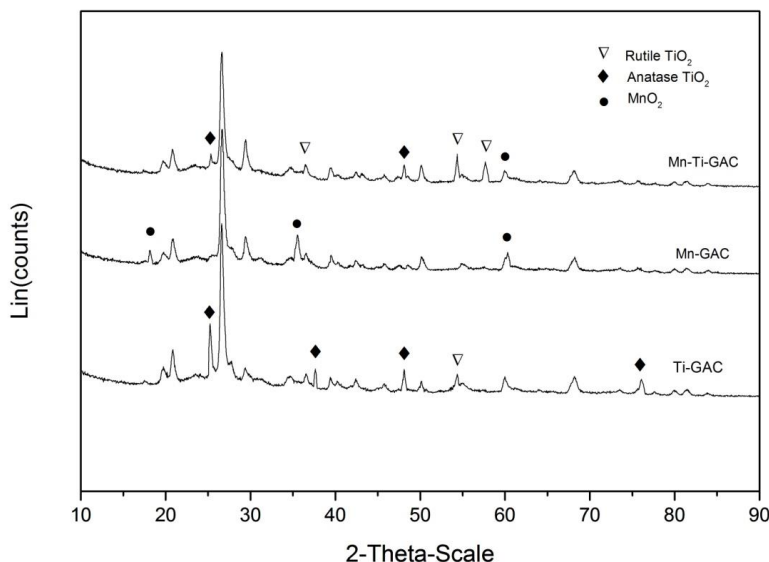


Figure 2. XRD diffraction patterns of CPEs.

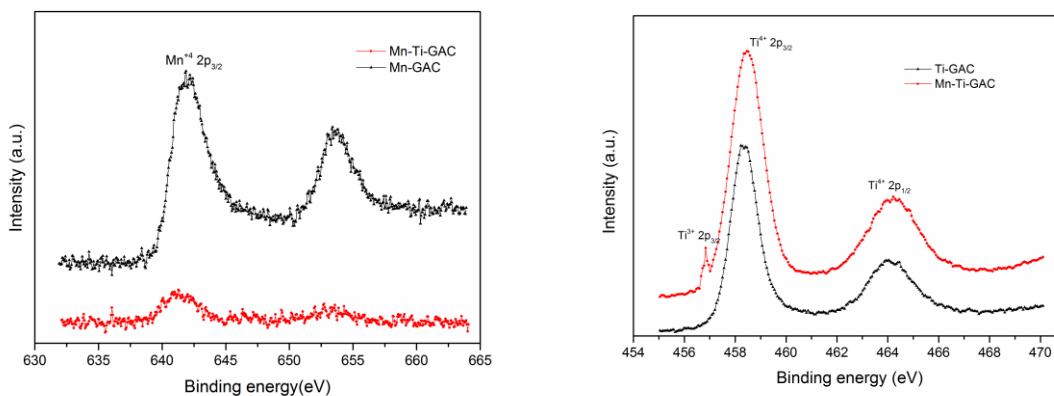
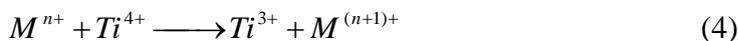
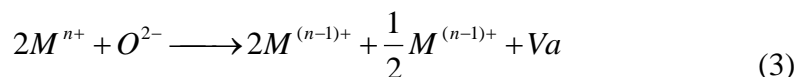


Figure 3. XPS spectra of different CPEs.

To further verify the conclusions of the XRD results and explore the surface composition and chemical states of the catalysts, the GAC-based electrodes were characterized by XPS. As shown in Fig. 3, the XPS peak positions of Ti 2p_{3/2} and Ti 2p_{1/2} are located at 458.45 eV and 462.48 eV, respectively. These results indicate that the Ti originating from TiO₂ in both Ti-GAC and Mn-Ti-GAC mainly exists as Ti⁴⁺ in the stoichiometric oxide TiO₂. It is noteworthy that there is an obvious fitting peak at 456.91 eV, which indicates the existence of Ti³⁺ in TiO₂ nano-particles (via Reaction (3) and (4)). The presence of Ti³⁺ in MnO₂-doped TiO₂ causes lattice distortion and results in the formation of oxygen vacancies. Therefore, the number of active sites increases and the catalytic efficiency of MnO₂-doped TiO₂ is improved. The position of the Mn 2p_{3/2} peak in the XPS spectra is similar to that in Mn-Ti-GAC (641.27 eV) and Mn-GAC (642.35 eV), thereby confirming the existence of Mn⁴⁺ in the

catalyst. Metallic manganese inhibits the phase transition of Ti, and multiple charged valence state metal cations promote redox reactions on the TiO₂ surface via Reactions (3) and (4) [20].



3.2 Treatment performance of the CPEs

The NFC treatment performance of the different CPEs in the 3DEF system was investigated, and the results are shown in Fig. 4(a). As seen, 21.82 % of the COD was removed in 120 min when no CPEs were present in the 3DEF system. However, 64.05 % of the COD was removed after GAC was added to the system as a particle electrode. This result further supports the conclusion of previous studies, which showed that 3DEF systems with particle electrodes have higher degradation efficiencies and improved electrochemical properties than 2DEF processes. Compared with the other CPEs, the COD removal efficiency of Mn-GAC (71.98 %) was lower than either Ti-GAC (73.22 %) or Mn-Ti-GAC (81.80 %). Clearly, Mn-Ti-GAC demonstrated the best catalytic activity. The COD removal efficiency differed insignificantly between 100 min (80.08 %) and 120 min (81.80 %); thus, a reaction time of 100 min was chosen for the subsequent experiments.

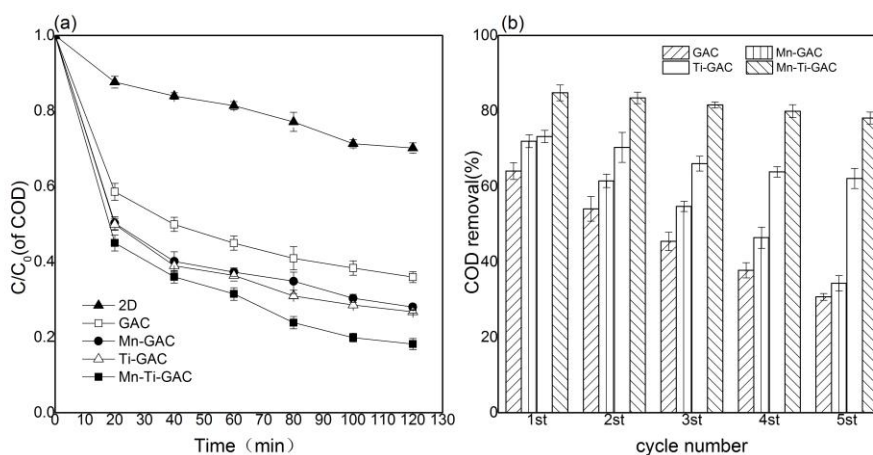


Figure 4. COD removal performance of the 3DEF system with different CPEs and cycling times. Experimental conditions: temperature, 25 °C; current density, 20 mA/cm²; CPE concentration, 100 g/L; Fe²⁺ concentration, 1.2 mM; pH 3; plant distance, 11 cm.

All CPEs were used five times to investigate the effects of cycling time on their performance. After the CPEs were reused once, they were washed several times with distilled water and added to the NFC to re-establish adsorption equilibrium. Fig. 4(b) shows the COD removal rate after 100 min with five cycles of various CPEs. The COD removal efficiency of the 3DEF system filled with GAC decreased from 64.05 % to 30.72 %, but it remained higher than that of the 2DEF system. The COD

removal efficiency of Mn-GAC CPE decreased significantly as the cycle time increased. That is, the removal rate decreased from 71.98 % to 61.45 % after the second cycle, and fell to 34.33 % after five cycles. This drop could be attributed to an acute outflow of the catalyst from the Mn-GAC CPE surface [21]. The electrocatalytic property of the Ti-GAC and Mn-Ti-GAC CPEs remained relatively stable, with COD removal efficiencies of 49.11 % and 62.14 %, respectively. Compared with the first cycle, the decreases in the COD removal rate of the Ti-GAC and Mn-Ti-GAC CPEs were 32.93 % and 26.72 %, respectively. Apparently, formation of the $\text{MnO}_2\text{-TiO}_2$ solid solution reduced dissolution of the catalyzing nano-particles.

3.3 Catalytic activity

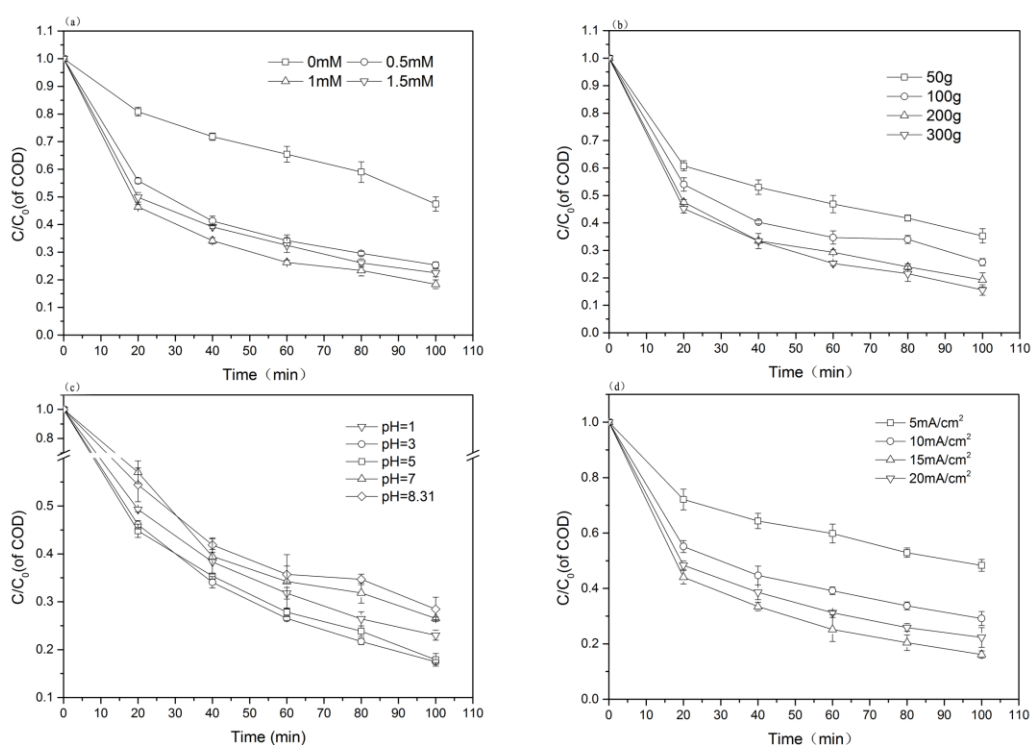


Figure 5. Effects of process parameters on the COD removal efficiency. (a) Fe^{2+} concentration, (b) CPE concentration, (c) pH, and (d) current density. Experimental conditions: (a) temperature, 25 °C; current density, 20 mA/cm²; CPE concentration, 100 g/L; pH 3; plant distance, 11 cm; (b) temperature, 25 °C; current density, 20 mA/cm²; pH 3; Fe^{2+} concentration, 1 mM; plant distance, 11 cm; (c) temperature, 25 °C; current density, 20 mA/cm²; CPE concentration, 200 g/L; Fe^{2+} concentration, 1 mM; plant distance, 11 cm; and (d) temperature, 25 °C; CPE concentration, 200 g/L; Fe^{2+} concentration, 1 mM; pH 3; plant distance, 11 cm.

3.3.1 Effect of Fe^{2+} concentration

One of the main degradation mechanisms of organic matter in a 3DEF system occurs via the Fenton reaction, and the Fe^{2+} concentration plays a significant role in the formation of $\cdot\text{OH}$. The COD

removal efficiency for different Fe^{2+} concentrations is shown in Fig. 5(a). In the absence of Fe^{2+} , the COD removal efficiency was only 66.57 % at the end of treatment. In consideration of the GAC adsorption equilibrium before the addition of Fe^{2+} to the system, this low efficiency may result from the existence of Fe^{3+} in the NFC, which is a reagent for the Fenton reaction via Reaction(2). Notably, the removal efficiency of COD was 74.66 % and 81.6 % when the Fe^{2+} concentration was 0.5 mM and 1 mM, respectively. When the Fe^{2+} concentration increased above 1 mM, however, the removal efficiency decreased to 77.51 %. This result is attributed to the formation of $\text{Fe}(\text{OH})_3$ flocs by extraneous Fe^{2+} species present in the system, which decreased the number of active sites on the cathode and CPEs for producing H_2O_2 [22]. Compared with the Fe^{2+} concentration used to treat NFC with 2D/F systems (3.68 mM) [23], a much smaller quantity of Fe^{2+} (1 mM) was used in the present study, which suggests that the 3DEF system possesses sufficient reactivity to regenerate Fe^{2+} . Indeed, a small quantity of Fe^{2+} formed complexes of iron with organic matter, suggesting that the concentration of dissolved Fe^{2+} and Fe^{3+} remained at a high level in the 3DEF system.

3.3.2 Effect of initial pH

The 3DEF system filled with Mn-Ti-GAC was examined at various solution pH values (1, 3, 5, 7, and the natural pH of NFC) to investigate the effect of the initial pH on the COD removal efficiency. As shown in Fig. 5(b), the optimum initial pH was 3 (82.55 %). At the extremely low pH of 1, the COD removal efficiency decreased to 77.00 % because $[\text{Fe}(\text{H}_2\text{O}_2)_6]^{2+}$ species formed, which react more slowly with peroxide than $[\text{Fe}(\text{OH})(\text{H}_2\text{O})_5]^{2+}$ [24]. When the pH was lower than 3, the electro-generated H_2O_2 reacted with hydrogen ions to form H_3O_2^+ via the reaction $\text{H}_2\text{O}_2 + \text{H}^+ \rightarrow \text{H}_3\text{O}_2^+$. The product H_3O_2^+ is a stable electrophilic that decreases the removal efficiency of COD [25]. The COD removal efficiency did not decrease significantly when the pH was increased from 5 to 7 to 8.31, as evidenced by values of 82.13 %, 73.49 %, and 71.56 %, respectively. The efficiency was lower at higher pH because relatively more $\text{Fe}(\text{OH})_3$ precipitate formed, which decreased the number of H_2O_2 -producing active sites on the cathode. Nevertheless, the heterogeneous EF reaction occurred on the surface of the nano-iron catalyst, thereby expanding the working pH range. Compared with the traditional Fenton process, the 3DEF system generates H_2O_2 on the surfaces of both the anode and the CPEs, avoiding degradation of H_2O_2 . Instead, H_2O_2 is catalytically decomposed to hydroxyl radicals by the enhanced specific surface area and the catalysts provided by the CPEs. Therefore, the 3DEF system showed high efficiency across a wide pH range.

3.3.3 Effect of CPE concentration

CPEs expand the reaction area of the 3D system via polarization under external electric fields. Fig. 5(c) shows the effects of CPE concentration on the treatment efficiency. As seen, the COD removal efficiency rose from 64.73 % to 84.43 % as the CPE concentration increased from 50 g/L to 200 g/L. However, the corresponding increase in efficiency was minimal (at only 3.67 %) when the CPE concentration was increased from 200 g/L to 300 g/L. The particle electrodes act as a micro-

electrolytic cell in which H₂O₂ is generated and the pollutants are oxidized. Although increasing the CPE concentration produced more H₂O₂ and made more catalytic sites available, a short-circuit current formed, which was enhanced by the addition of high amounts of CPEs, the net result of which is to decrease the current and degradation efficiencies [26]. Thus, 200 g/L of the Mn-Ti-GAC electrodes was selected for use in subsequent experiments.

3.3.4 Effect of current density

Current density reflects the rate of anodic oxidation and determines the degree of polarization of the particle electrodes. Current densities ranging from 5 mA/cm² to 20 mA/cm² were selected to investigate its effect on the degradation of COD (Fig. 5(d)) As seen, the removal of COD increased initially but then decreased as the current density increased. The COD removal efficiency increased from 54.65 % to 83.84 % as the current density rose from 5 mA/cm² to 15 mA/cm². However, it dropped to 77.68 % when the current density increased further to 20 mA/cm². According to Faraday’s law, the production of ·OH, Cl₂, and H₂O₂ increase as the current density increases. However, excessively high current density accelerates the evolution of hydrogen and oxygen, and excessive current density accelerated the electro-generation of H₂O₂, which had an adverse effect on the degradation efficiency because of its ability to scavenge radicals. For these reasons, a current density of 15 mA/cm² was chosen in further studies.

3.4 Changes in major pollutants in the 3DEF system under optimal conditions

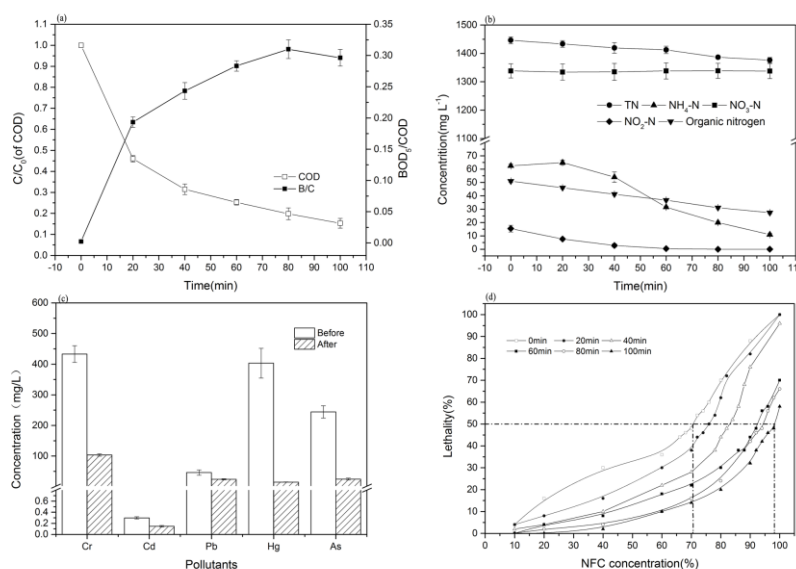


Figure 6. Change in the major pollutants of the NFC. (a) COD and BOD₅/COD, (b) nitrogen pollutants, (c) metals (Cr, Cd, Pb, Hg, and As), and (d) biotoxicity. Experimental conditions: temperature, 25 °C; current density, 15 mA/cm²; CPE concentration, 200 g/L; pH 3; Fe²⁺ concentration, 1 mM; plant distance, 11 cm.

3.4.1 Organic matter removal and distribution of the DOM fractions

As indicated in Fig. 6(a), the COD removal efficiency reached 84.68 % under optimal conditions. In this case, the initial NFC concentrate contained only 11.37 mg/L of BOD₅, which led to the poor biodegradability observed for the initial NFC (i.e., the BOD₅/COD was only 0.002). The biodegradability of the effluent was improved through the 3DEF system filled with Mn-Ti-GAC particles. The BOD₅/COD increased to 0.296 at a treatment time of 100 min, a 99 % improvement.

The major organic component in the landfill concentrates is DOM. The DOM from the NFC was fractionated into HA, FA, and HyI in order to characterize the transformation of organic substances; the results are shown in Table 2. The FA fractions accounted for 55.27 % of the DOM in the NFC, and the HA and HyI fractions accounted for 22.26 % and 38.15 %, respectively. After treatment by the 3DEF system, the HA and FA concentrations were reduced to 62.76 mg/L and 194.87 mg/L, respectively, while their removal efficiencies reached 76.64 % and 78.85 %, respectively. However, the concentration of HyI decreased from 463.85 mg/L to only 388.74 mg/L. HA and FA can degrade into HyI, which may explain the poor HyI removal efficiency [7]. Additionally, the reaction rates of hydroxyl radicals with large organic molecules like HA and FA [$k = 10^9-10^{10}$ L/(mol·s)] are higher than that with HyI [27]. Hydroxyl radicals destroy aromatic structures and unsaturated bonds, generating a large number of hydrophobic species to be transformed into hydrophilic species. Thus, the increase in the BOD₅ benefited from the increase of the HyI fractions.

Table 2. DOM components in the NFC before and after the 3DEF treatment

DOM fraction	Before 3DEF		After 3DEF		Removal efficiency(%)
	Concentration(mg/L)	Percentage(%)	Concentration(mg/L)	Percentage(%)	
HA	272.91±22.26	16.51	62.76±4.97	9.71	76.64±2.86
FA	916.48±55.27	55.27	194.87±19.42	30.15	78.85±1.05
HyI	463.85±38.15	28.06	388.74±32.84	60.14	16.07±2.15

3.4.2 Nitrogen removal in the 3DEF system

The variation of different nitrogen forms during the 3DEF treatment is shown in Fig. 6(b). As seen, NH₃-N, NO₂-N, and organic nitrogen were effectively removed by the 3DEF system, with corresponding removal efficiencies of 81.3 %, 99.3 %, and 46.4 % at the end of the treatment, respectively. The concentration of NH₃-N increased in the first 20 min and then decreased. A slight increase of NH₃-N was observed since organic nitrogen can be oxidized to NH₃-N and NO₂-N. NH₃-N can be oxidized directly to N₂ at the anode and indirectly to NO₃-N and N₂ via chlorine/hypochlorite species in the electro-Fenton system [28]. Furthermore, the aeration system contributed to releasing NH₃-N and N₂ to the air. Therefore, NH₃-N was removed efficiently after 20 min.

$\text{NO}_3\text{-N}$ increased from 1348.25 mg/L to 1358.42 mg/L, indicating that a portion of the organic nitrogen, $\text{NH}_3\text{-N}$, and $\text{NO}_2\text{-N}$ were oxidized to $\text{NO}_3\text{-N}$. The removal efficiency of the total ammonia (TN) was only 4.84 %, as $\text{NO}_3\text{-N}$ occupied the major part of the TN concentration in the influent and effluent at the end of the 3DEF treatment.

3.4.3 Metal removal

As shown in Fig. 6(c), the 3DEF system is capable of efficiently removing metals. Among the five metals listed in the emission standard (Cd, Cr, Hg, Pb, and As), As and Hg had the highest removal efficiencies of 88.89 % and 96.28 %, respectively. At 47.58 %, Pb had the lowest removal efficiency. Notably, all the heavy metal levels meet the emission standards. Refractory organic matter such as HA and FA possess complex functional groups that strongly absorb heavy metals [7]. The degradation of organic matter would consequently lead to the release or transfer of metals, and the free metals would be removed by $\text{Fe}(\text{OH})_3$ generated by increasing the pH.

3.4.4 Acute toxicity assessment

The acute toxicity of the NFC to *Artemia salina* was conducted to assess biotoxicity. The 24h- LC_{50} acute toxicity of the NFC was 70.18 % before treatment by the 3DEF system (Fig. 6(d)), and the acute toxicity declined slowly in the first 40 min (23.7 %). According to Fig. 6(d), degradation-resistant species were oxidized to biodegradable components, which reduced the acute toxicity. At the end of the treatment, the 24 h- LC_{50} dropped to 98.11 %, demonstrating that the toxic components were degraded to less toxic or non-toxic components, or they were directly removed by the 3DEF system.

3.5 Reaction mechanism of organic pollutant degradation

Based on the experimental results, the 3DEF system equipped with Mn-Ti-GAC demonstrates superior treatment capabilities than the other CEPs examined. As described above, there are two pathways to oxidize organic matter in a 3DEF system. $\cdot\text{OH}$ plays a pivotal part in the degradation or mineralization of contaminants. Because tertiary butanol is an effective scavenger of $\cdot\text{OH}$, it is often used as an indirect measure of $\cdot\text{OH}$ generation in quantitative studies of electrochemical systems. Fig. 7 shows the COD removal efficiency of the NFC treated by different systems at different tertiary butanol concentrations. In the absence of tertiary butanol, a 4.17 % and 14.24 % decrease of COD removal efficiency was observed in the 2D and 3D-Mn-Ti-GAC systems, respectively, indicating that $\cdot\text{OH}$ was not responsible for the COD removal in the electrochemical systems and that particle electrodes packed in the electrochemical system could effectively improve $\cdot\text{OH}$ production.

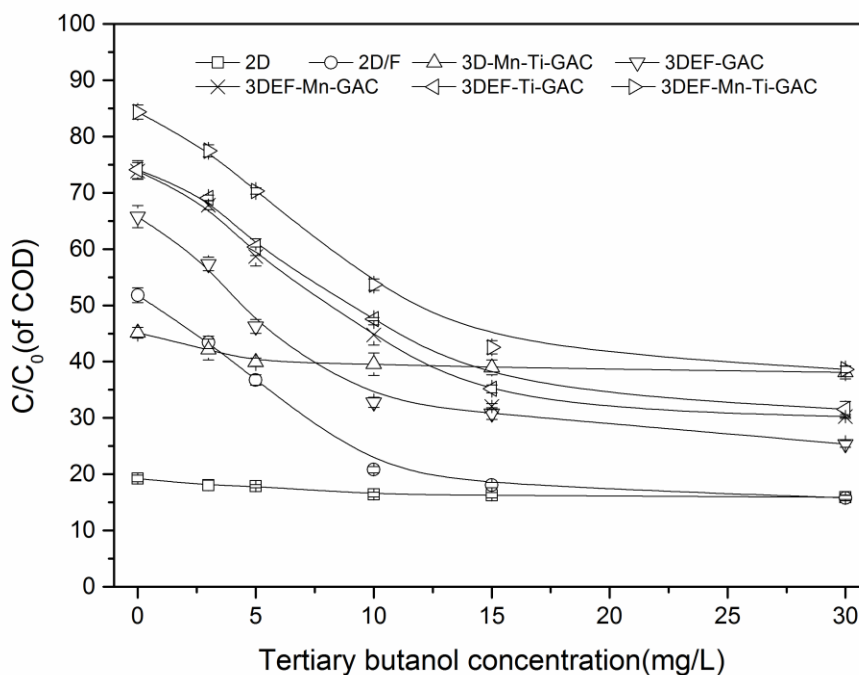
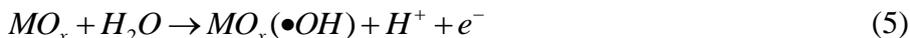


Figure 7. Degradation of COD with different processes under different tertiary butanol concentrations. Experimental conditions: temperature, 25 °C; current density, 15 mA/cm²; CPE concentration, 200 g/L; pH 3; Fe²⁺ concentration, 1 mM, plant distance, 11 cm.

Moreover, the addition of tertiary butanol critically affects the COD removal efficiency of electro-Fenton systems, especially for 2DEF systems. This demonstrates that $\cdot\text{OH}$ plays a major role in electro-Fenton degradation processes. When a small amount of tertiary butanol was added to the electro-Fenton systems ($\sim 0\text{--}5\text{ mg/L}$), the COD removal efficiency decreased significantly. This decrease was more significant in the 2D/F and 3DEF-GAC systems than that in the 3DEF system filled with GAC-based granular electrodes, which further confirms that GAC-based electrodes contribute to the generation of $\cdot\text{OH}$. Among all three GAC-based electrode particles, Mn-Ti-GAC exhibited the highest $\cdot\text{OH}$ activity in the presence of high concentrations of tertiary butanol ($\sim 10\text{--}15\text{ mg/L}$), which can be ascribed to the unique physical appearance of MnO₂-doped TiO₂. Under an excessively high tertiary butanol concentration (30 mg/L), the treatment efficiency of the 3D-Mn-Ti-GAC (72.15%) and 3DEF-Mn-Ti-GAC (71.36%) systems was better than the other systems examined.

Given these results, we propose a possible reaction mechanism to explain the degradation of organic pollutants in the 3DEF system with Mn-Ti-GAC. First, macromolecule organic matters (HA and FA) were adsorbed into mesopores of the GAC-coated particles. Then, benefiting from oxygen vacancies on the Mn-Ti-GAC particle surface, the “non-active” electro-catalyst metal oxide (MO_x) easily decomposes to form strong oxidants, such as MO_x($\cdot\text{OH}$) species (Reaction (5)) [29]. The adsorbed $\cdot\text{OH}$ is not easy to be consumed by oxygen evolution because of these strong oxidizing intermediate. It will contribute to increase utilization ratio of $\cdot\text{OH}$. MO_x($\cdot\text{OH}$) and $\cdot\text{OH}$ generated from the Fenton reaction (Reaction (2)) non-selectively oxidize and mineralize these refractory substances

to micromolecular organic or CO₂ species (Reactions (6) , (7) and (8)) [15,30]. Conjugated chromophore and aromatic structure on humic substances were electrolyzed and oxidized to innocuous small molecule products. Concomitantly, these products rapidly transfer to either the micropores or liquor, which further promotes the catalytic rate. The net effect of these processes is that the effluent possesses a high (BOD₅)/COD and low toxicity.



4. CONCLUSIONS

In this study, a MnO₂-doped TiO₂-coated GAC was prepared by a one-step sol-gel method and subsequently used to enhance the electrochemical oxidation of nanofiltration concentrates (NFC) from landfill leachate. We showed that the efficiency and service life of the Mn-Ti-GAC catalytic particle electrode (CPE) are higher than those of conventional CPEs. The optimal operating parameters of the three-dimensional electro-Fenton (3DEF) system were determined to include a current density of 15 mA/cm², Fe²⁺ concentration of 1 mM, initial pH of 3, and CEP concentration of 200 g/L. Under these optimal conditions, the removal efficiencies of COD and NH₃-N were 84.68 % and 81.3 %, respectively. The (BOD₅)/COD increased from 0.002 to 0.296, thereby providing an attractive basis for biotreatment application. Overall, the 3DEF treatment method described herein is an effective approach to reduce the toxicity of NFC. Indeed, the results of this study indicate that 3DEF systems filled with Mn-Ti-GAC CEP are an effective method for treating NFC.

ACKNOWLEDGEMENTS

This work was financially supported by the Water Pollution Control and Management Key Project of Science and Technology of China with Grant No. 2014ZX07202-011, the National Natural Science Fund of China with Grant No. 51508342, the China Environmental Protection Foundation "123 Project" with Grant No. CEPF2014-123-1-3, and the Liaoning Province Doctoral Scientific Research Foundation with Grant No. 201501069.

References

1. B.Tiago, B.B. Jean, Z.S. Fernanda, M.D. Tamires, S. Jacira and T.P. Claus, *Environ. Toxicol. Phar.*, 28 (2009) 288.
2. A. Fernandes, M.J. Pacheco, L. Ciraco and A. Lopes, *Appl. Catal. B: Environ.*, 176-177 (2015) 183.
3. V. Michel, V.M. Ruben, P.G. Dorian, A. Bernardo, F.U. Jorge and G. Ibanez, *J. Hazard. Mater.*, 205-206 (2012) 208.
4. M. El-Fadel, F. Sleem, J. Hashisho, P.E.Saikaly, I.Alameddine and S.Ghanimeh, *Waste. Manage.*, 73 (2018) 165.

5. G.R. Beatriz, L.S. Amanda, P.T.T. Luiza, A.O. Adriana, C.L. Liséte and C.S.A. Miriam, *Waste Manage.*, 70 (2017) 170.
6. D. Davor, K. Krešimir and S. Tea, *Sep. Purif. Technol.*, 168 (2016) 39.
7. R. He, B.H. Tian, Q.Q. Zhang and H.T. Zhang, *Waste Manage.*, 38 (2015) 232.
8. Q.Q. Zhang, B.H. Tian, X. Zhang, A. Ghulam, C.R. Fang and R. He, *Waste Manage.*, 33 (2013) 2277.
9. S. Ismail and A. Tawfik, *Int. Biodeter. Biodegr.*, 111 (2016) 22.
10. H. Wang, Y.N. Wang, X. Li, Y. Sun, H. Wu and D. Chen, *Waste Manage.*, 56 (2016) 271.
11. B. Zhou, Z. Yu, Q. Wei, H. Y. Long, Y. Xie and Y. Wang, *Appl. Surf. Sci.*, 377 (2016) 406.
12. C. Zhang, Y.H. Jiang, Y.L. Li, Z.X. Hu, L. Zhou and M.H. Zhou, *Chem. Eng. J.*, 228 (2013) 455.
13. I. Sirés, J.A. Garrido, R.M. Rodriguez, E. Brillas, N. Oturan and M.A. Oturan, *App. Catal. B: Environ.*, 72 (2007) 382.
14. M. Giuseppe, P. Michele, F. Debora, C. Simone, M.Y. Michail and L. Antonella, *J. Environ. Manage.*, 203 (2017) 817.
15. X. Li, Y. Wu, W. Zhu, F. Yue, Y. Qian and C. Wang, *Electrochim. Acta.*, 220 (2016) 276.
16. M. Mehrjouei, S. Müller and D. Möller, *Environ. Prog. Sustain. Energy.*, 33 (2014) 178.
17. R.P. Aline, R.E. Fernando, C.D. Isabella, E.G.T. Daniela, N.M. Aparecido, R. Caroline, H.B. Fernando and D.K. Alexander, *J. Environ. Chem. Eng.*, 5 (2017) 5448.
18. J. Liu, J.S. Ye, Y.F. Chen, C.S. Li and H.S. O, F. Ji, C. Li, L. Deng, *Chemosphere.*, 190 (2018) 225.
19. APHA, AWWA, WEF, *American Public Health Association (EDs.)*, New York. 1998.
20. V. Michel, V.M. Ruben, P.G. Dorian, A. Bernardo, F.U. Jorge and G. Ibanez, *J. Hazard. Mater.*, 205-206 (2012) 208.
21. F. Zhang, G.M. Li, Y. Sheng and J. Ji, *Environ. Sci.*, 28 (2007) 1715.
22. C.T. Wang, J.L. Hu, W.L. Chou and Y.M. Kuo, *J. Hazard. Mater.*, 152 (2008) 601-606.
23. Y. Wang, X. Li, L. Zhen, H. Zhang and Y. Zhang, *J. Hazard. Mater.*, 229-230 (2012) 115.
24. H. Gallard, J. Laat and B. Legube, *New. J. Chem.*, 22 (1998) 263.
25. S. Mohajeri, H.A. Aziz, M.H. Isa, M.A. Zahed and M.N. Adlan, *J. Hazard. Mater.*, 176 (2010) 749.
26. B. Hou, H. Han, S. Jia, H. Zhuang, P. Xu and K. Li, *J. Taiwan. Inst. Chem. Eng.*, 60 (2016) 352.
27. M.E. Lindsey and M.A. Tarr, *Chemosphere.*, 41 (2000) 409.
28. M. Emmanuel, P. Steve and P. Marie-Noëlle Pons, *Chemosphere.*, 201 (2018) 6.
29. X.Y. Li, J. Xu, J.P. Cheng, L. Feng, Y.F. Shi and J. Ji, *Sep. Purif. Technol.*, 187 (2017) 303.
30. B. Correalozano, C.H. Comninellis and A. D. Battisti, *J. Appl. Electrochem.*, 26 (1996) 683.